BULLETIN OF THE POLISH ACADEMY OF SCIENCES
TECHNICAL SCIENCES, Vol. 70(1), 2022, Article number: e140354
DOI: 10.24425/bpasts.2022.140354

The gyrotron for DNP-NMR spectroscopy: A review

Kacper NOWAK*

Wroclaw University of Science and Technology, Wybrzeże Wyspiańskiego 27, 50-370 Wrocław, Poland

Abstract. This paper outlines the principle of the DNP-NMR technique. The gyrotron, as a very promising microwave source for NMR spectroscopy, is evaluated. Four factors: power stability, power tuning, frequency stability, and frequency tuning determine the usability of the gyrotron device. The causes of instabilities, as well as the methods of overcoming limitations and extending usability are explained with reference to the theory, the numerical and experimental results reported by gyrotron groups.

Key words: DNP-NMR spectroscopy; gyrotron stability; gyrotron tuning.

1. INTRODUCTION

Nuclear magnetic resonance (NMR) spectroscopy is a very powerful scientific tool. It has wide applications in chemistry [1], medicine [2], biology [3] and material physics [4], as it provides atomic level information on the molecular structure. The most common applications include the structural analysis of molecules, biomolecules, proteins [5, 6], bionucleic acids (RNA), deoxyribonucleic acids (DNA) and material science. Other interesting applications include food science [7] (composition analysis and the measurement of the physicochemical properties and functionality of food matrices), falsified or illegal drugs analysis [8], cancer detection [9], and personalized medical treatment [10]. All the mentioned applications use the NMR method as a key analysis tool, and therefore the importance of NMR spectroscopy is unprecedented.

The NMR experiment itself is very time consuming and requires many technical difficulties to be overcome, and therefore many techniques have been employed to enhance its usability and decrease measurement time.

Software techniques, such as advanced data analysis of NMR data sets – deep learning techniques (DL) [11] – are being employed. Three basic architectures of neural networks are in use in Deep Neural Networks (DNNs) [12], Convolutional Neural Networks (CNNs) [13, 14] and Recurrent Neural Networks (RNNs) [15]. The main purposes of using DL techniques are: reconstruction of the spectra, to accelerate the acquisition of experimental data, denoising of the spectra, chemical shift prediction, and automated peak picking.

The key method to increase signal strength is the Dynamic Nuclear Polarization (DNP) technique. It is based on the physical phenomena of the polarization transfer from hyperpolarized electrons to the nuclei. This method requires special hardware to be developed, but offers much higher signal strength and shorter experiment times when compared to NMR.

*e-mail: kacper.nowak@pwr.edu.pl

Manuscript submitted 2021-09-01, revised 2021-11-10, initially accepted for publication 2021-11-18, published in February 2022.

A wide range of techniques is applied to make NMR phenomena more usable and applicable in science, but this paper is focused on a microwave source – the gyrotron [16–19] – used in the application of DNP-NMR.

2. NMR MECHANISM

The NMR experiment is applicable to any kind of sample that contains nuclei possessing spin. Any motion of a charged particle (rotation in this case) has an associated magnetic field around it, which means that a magnetic dipole is created. A magnetic moment μ of a nucleus is connected with its spin angular momentum. In classical mechanics, this is expressed by the equation $\mu = \gamma I$, where I is the angular momentum quantum number, called nuclear spin, and γ is a proportionality constant – gyromagnetic ratio. Every magnetic dipole placed in a strong magnetic field will experience Larmor precession [20], and it will spin around magnetic lines, however classic theorem is not appropriate to describe NMR phenomena.

In quantum mechanics, the description of intrinsic(nuclear) angular momentum P is quantized as:

$$P = \hbar\sqrt{I(I+1)}\,, \tag{1}$$

where: $\hbar$ – the reduced Planck's constant, and I – nuclear spin.

The nuclear spin quantum number can have values $I = 0, 1/2, 1, 3/2, 2, \ldots 7$. It is an intrinsic property of the particle, and is where the quantization comes from. The difference in the energy level between spin resonance states is proportional to the magnetic field strength B_0 and is defined by the equation:

$$\Delta E = \gamma\hbar B_0\,, \tag{2}$$

where: $m_I = -I, -I+1, ..., I-1, -I$ in the range of $\langle -I, +I\rangle$, which defines the magnetic quantum number. For ^1H nuclei $I = \frac{1}{2}$ there are two spins $m_I = \left(+\frac{1}{2} \text{ and } -\frac{1}{2}\right)$. This condition is presented in Fig. 1.

In the NMR experiment, a strong magnetic field B_0 is delivered from a magnet, and a weak field B_1 is supplied by radio

© 2022 The Author(s). This is an open access article under the CC BY license (http://creativecommons.org/licenses/by/4.0/)

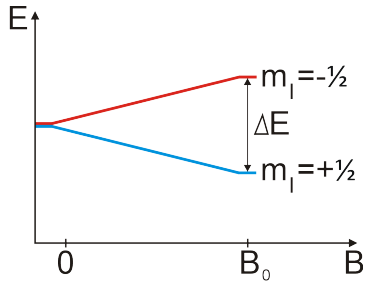

Fig. 1. Nuclear spin energy levels for spin $m_I = -\frac{1}{2}$ and $m_I = +\frac{1}{2}$

frequency (RF) radiation. NMR active nuclei absorb electromagnetic radiation at a characteristic frequency causing transition between the lower energy level and the upper energy level Fig. 1. The population between two spin states is in imbalance. When the RF pulse is turned off, the population between two spin states returns to equilibrium and free induction decay is observed. This is the **N**uclear **M**agnetic **R**esonance response that is measured. Unfortunately, this is a very weak signal and requires sensitive RF receivers and for the measurement to be repeated multiple times. The spectrum from a decay has a low signal to noise ratio (SNR) and only grows with $\sqrt{N}$, where N is the number of repetitions of the experiment at one frequency [21]. Preserving the same experimental conditions for a long time is a very challenging task.

The sensitivity of the NMR experiment is determined by the energy difference equation (2), because this determines the population of spin states. Therefore, the SNR is proportional to the polarization P and is usually determined by the Boltzmann law at thermal equilibrium:

$$P = \frac{n_\beta - n_\alpha}{n_\beta + n_\alpha} = \tanh\left(\frac{\gamma\hbar B_0}{2k_B T}\right), \tag{3}$$

where: n_α and n_β – the population of two spin states, T – temperature K.

Equation (3) reveals the limitations of NMR. The strongest commercial 1.2 GHz Bruker NMR was reported in May 2020 to be installed at the University of Florence's CERM research center. The system cost 17.8 million US dollars. The world's strongest NMR is capable of 1.5 GHz and is installed at the US National High Magnetic Field Laboratory. According to equation (4), for proton ^1H nuclei and a frequency of 1.5 GHz, the magnetic field is $B_0 = 35.23$ T, and yet with such a powerful device equation (3) reveals that polarization is still only 0.0122% at room temperature of 23°C.

The conclusion is that the SNR is proportional to polarization $SNR \sim P$, and can be improved by applying a higher magnetic field, increasing the gyromagnetic ratio, or lowering the temperature. To change the temperature or magnetic field, expensive equipment needs to be employed. Moreover, the gyromagnetic ratio is the property of the nuclei, so it cannot be changed. Just a few years after NMR was invented, Overhauser published (in 1953) work describing the polarization coupling phenomena (DNP) between nuclei and free electrons in metals [22].

3. DNP TECHNIQUE

The DNP-NMR technique belongs to the hyper-polarization family and is applied to solids, liquids and gas measurements. The general principle of DNP is that a higher level of polarization of the electron spins can be transferred to the surrounding nuclear spins upon microwave irradiation at or near the electron paramagnetic resonance (EPR) transitions. However, polarization transfer from electrons to nuclei is a complex phenomenon. Many different polarization transfer mechanisms exist: Solid Effect (SE), Overhauser Enchancement (OE), Cross Effect (CE), Thermal Mixing (TM) [2, 23–26]. These mechanisms can occur alone or simultaneously, depending on the substance's properties.

Despite different underlying physics phenomena, several experimental approaches to DNP-NMR can be applied [27]. For solid states, Magic Angle Spinning (MAS-DNP) is routinely performed and requires continuous wave irradiation generated by an external, strong microwave source. The microwave frequency has to be close to the electron spin resonance frequency of the investigated particle in the magnetic field [21]. To study liquid state substance dissolution, DNP (d-DNP) is the most common method. By applying methods developed for solids and liquids, gas substances can be measured, e.g. low temperature MAS-DNP of frozen gas can be performed [28], dissolution DNP can be applied [29], or even imaging of low pressure gas is possible [30].

The equation that allows the microwave frequency (Larmor frequency) required for the experiment to be calculated, in classic mechanical physics, is defined as $\omega_L = \frac{eB_0}{2m}$. This equation does not hold in quantum mechanics, and therefore the Larmor frequency has to be defined as:

$$\omega_L = \frac{eB_0}{2m} g = |\gamma| B_0, \tag{4}$$

where e – a unit charge, m – the particle mass, and g the g-factor (dimensionless magnetic moment).

If NMR with the strongest magnet in the world is considered, then $B_0 = 35.23$ T, and the Larmor frequency for the proton $f_{Lp} = \frac{\omega_{Lp}}{2\pi} = 1.5$ GHz and for the electron $f_{Le} = \frac{\omega_{Le}}{2\pi} =$ 987 GHz. To polarize protons, the RF signal can by easily generated by electronics, but in the case of the DNP-NMR, the microwave signal must have a frequency close to the electron Larmor frequency for energy transfer to occur, and therefore applicable sources are very limited. Millimeter wave generators such as the extended interaction oscillator (EIO) or backward wave oscillator (BWO) rely on fragile slow-wave structures to generate microwave radiation, and therefore they have a limited operating lifetime at the high power levels required for the DNP experiment. For these reasons cyclotron resonance masers (CRM) – Gyrotrons – are the most reasonable choice for generating radiation at high a frequency (100–1000 GHz) and 10–50 W power level.

The electron spin has much larger polarization due to the significantly higher gyromagnetic ratio of the electron when compared to the proton or other nuclei, and as we have men-

tioned before, $SNR \sim P$. The gyromagnetic ratio of a particle or a system is the ratio of its magnetic moment to its angular momentum. Let us compare the proton and electron gyromagnetic ratio:

$$\frac{\gamma_p}{2\pi} \approx 43 \left[\frac{\text{MHz}}{\text{T}}\right], \quad \frac{\gamma_e}{2\pi} \approx 28 \left[\frac{\text{GHz}}{\text{T}}\right], \quad \frac{\gamma_e}{\gamma_p} \approx 658. \tag{5}$$

Equation (5) defines the maximum theoretical gain that can be obtained using the DNP technique [25,31]. Now, using equation (3) at temperature 23°C and $B_0 = 35.23$ T, the proton polarization is $P_p = 0.0122\%$, and $P_e = 8.0076\%$ is for the electron. Experiments reported in the literature show that the real-life enhancement factor is: ≈ 80 for 284 MHz DNP-NMR (reduced thermal noise at temperature 90 K) [32], ≈ 60 for 400 MHz DNP-NMR, ≈ 50 for 500 MHz DNP-NMR [33], and ≈ 30 for 700 MHz DNP-NMR. This is why the DNP technique is so important, and it justifies the importance of the development of high frequency gyrotrons.

4. GYROTRONS IN THE NMR EXPERIMENT

A gyrotron extracts RF power from the perpendicular energy of an annular helical electron beam that is released by an electron gun and guided by a magnetic field [34]. The initial energy of the electron is determined by the gun's cathode voltage. The RF field interacts with electrons in the microwave cavity. The electron's trajectory and standing wave inside the cavity are designed in such a way that cyclotron radiation phenomena occurs. In a successfully designed device, more electrons slow down (lose energy) than speed up (gain energy), and therefore the total energy balance is in the favor of the RF field enhancement. In the described condition, microwave radiation is observed at the output.

To successfully employ a continous wave (CW) gyrotron as a RF source for NMR-DNP spectroscopy, several factors need to be taken into account:

- A specific operation frequency of 263, 394, 460, 527, 650 GHz and higher,
- output power of 10–100 W,
- a minimum frequency stability of 10^{-5}, power stability 1%,
- high spectral purity,
- reliable operation for days – long-term stability,
- frequency tuning (adjustment) ∼1 GHz is desirable,
- wide-range frequency tuning to cover many DNP experimental configurations with one device is desirable,
- "turn-key" operation determines usability.

Important factors that researchers focus on the most are frequency stability and the tuning range.

There are three crucial ways to change a gyrotron's operating frequency. They are based on the operation principle, and are successfully tested in NMR experiments:

- cathode voltage tuning,
- anode voltage tuning,
- magnetic field tuning.

There are also two methods that are proposed and investigated, but are not commonly used. These methods are:

- temperature control – variation of cavity dimension,
- movable internal insert in a coaxial gyrotron.

As an outcome of the requirements, a compromise has to be made. High order modes are closely spaced (similar characteristic values), which results in smoother frequency tuning when changing the operating mode, as well as lower ohmic losses, because most of the energy is placed further from the resonator wall. A longer cavity is required by low voltage gyrotrons, as electrons are weakly relativistic, and it is therefore required to increase the time of interaction between the electrons and microwave RF field. A longer cavity will increase ohmic losses, because the wave has to travel a longer distance inside the waveguide. Each reflection from the wall will disperse energy. On the other hand, a long cavity will provide smoother frequency tuning (the frequency of following modes will be more similar to each other). To reach the THz range, second or third harmonic operation is a must, because it lowers the requirement for the magnetic field by a factor of two (second harmonic) or three (third harmonic). However, the required magnetic field value is still very high, but possible to achieve. As a final result, the efficiency of the gyrotron drops significantly and the frequency tuning range narrows, but they remain reasonable enough to make the gyrotron the best candidate for the RF source in the application of DNP.

4.1. Cathode voltage – the frequency tuning method

Frequency and power modulation are useful for extending a gyrotron's applications to fields like communication and scientific measurements. Rapid frequency modulation by changing the cathode voltage was described theoretically and verified experimentally in [35]. The principle is that by varying the cathode voltage V_c (accelerating voltage), the beam velocity is changed, which results in a change of the electron mass and then in the modulation of cyclotron frequency. The modulation obtained is 20 MHz, with an efficiency of $\frac{\Delta f}{\Delta V_c} = 0.25 \frac{\text{MHz}}{\text{V}}$. A limiting parameter is the resonant cavity quality factor Q, which restricts the operating frequency [36].

High speed frequency modulation of a 460 GHz gyrotron for 700 MHz DNP-NMR was demonstrated in [37]. Modulation frequency $f_m < 10$ kHz of the cathode voltage $\delta V_c = 1$ kV

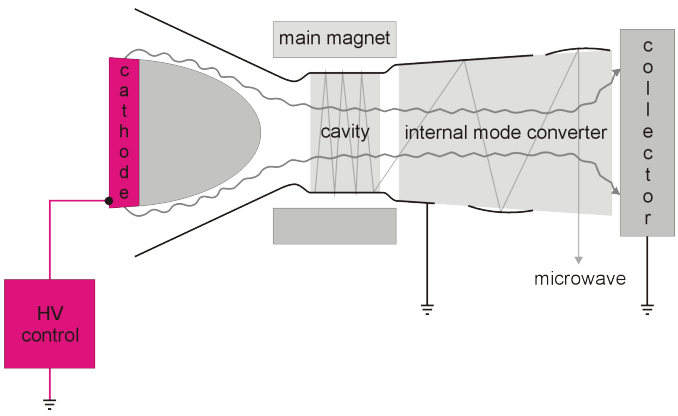

Fig. 2. Cathode voltage control mechanism. Cathode and high voltage power supply marked in color are used for controlling frequency

peak-peak produced modulation of the gyrotron's microwave frequency $\delta f = 53$ MHz at $f = 460$ GHz. A further increase of the gyrotron's modulation frequency is limited by the effect of the frequency pulling by the resonant cavity. It is reported that a gyrotron cannot follow cathode modulation frequencies f_m higher than 20 kHz, as output modulation frequency decreases. The authors have also investigated frequency tuning in the function of the modulation voltage. In this case triode type electron gun was used as shown in the Fig. 8. Experiment results show that it is 50 MHz/kV. High speed modulation of the cathode voltage also allows stabilization using the PID feedback circuit.

In paper [38], it is described that frequency tuning is achieved by changing the cathode voltage under constant: magnetic field, anode voltage and gun coil current. Frequency was measured in the heterodyne detection scheme by injecting a signal to the mixer part as a 16th harmonic for down-conversion to intermediate frequency, which can be measured by a spectrum analyzer. In the presented system, variation of the magnetic field was not possible due to the threshold, and therefore fine tuning using the cathode voltage was performed. As a result, the frequency range $\langle 393.8 - 394.6 \rangle = 0.8$ GHz was achieved by varying the cathode voltage in the range $\langle 15.3 - 19 \rangle = 3.7$ kV, which leads to the conclusion that the tuning sensitivity factor was 216 MHz/kV.

In [39], a theoretical study on an ultralow-voltage gyrotron is reported. The device has a tuning range of 10.7 GHz at a frequency of 330 GHz by changing the cathode voltage in the range of $\langle 0.3 - 0.8 \rangle$ kV. In the simulation, efficiency and output power is evaluated. For a cathode voltage of 0.3 kV, current of 0.5 A and a helical electron beam, output power above 1 W is obtained. The authors report that the gyrotron at cathode voltage 0.6 kV can reach a peak efficiency of 17%, and for 0.3 kV – 9.6%. The main drawback of lowering the operating voltage is that the coupling between the electron beam and RF field decreases.

4.2. Magnetic field – the frequency tuning method

Frequency tuning with the magnetic field can be done in two manners. The first is step tuning, which means changing from one discrete frequency to another (from one cavity mode to another). There are narrow regions around each central frequency, where smooth tuning is observed. The second is continuous tuning, which is especially desired for spectroscopy as it simplifies

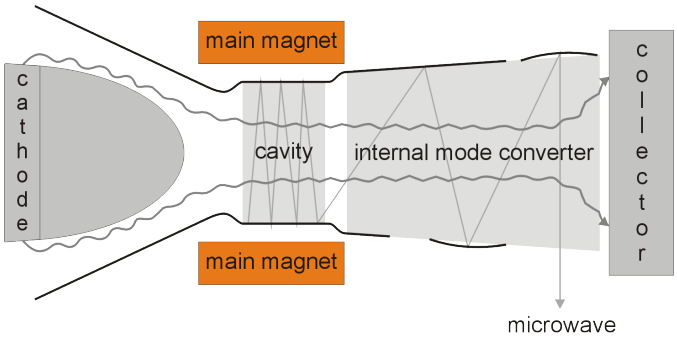

Fig. 3. Magnetic field control mechanism. Main magnet marked in color is used for controlling frequency

the spectrometer setup. This behavior is achieved by designing the cavity in such a way that closely spaced axial modes are exploited. The typical smooth (continuous) frequency tuning range for single mode operation is up to 3.3 GHz [40–46]. However, there is a large variation of the output power. The main limitation of the magnetic field method is a slow sweep rate due to the slow response of the cryomagnet and skin effect in the gyrotron body. This method is suitable for wide frequency tuning, but is not used for stabilization.

Frequency step tunability in the wide range, together with changing from first to second harmonic operation in one gyrotron device, is presented in [47]. The extended range of operating frequency is 150–300 GHz at the first harmonic and 300–600 GHz at the second harmonic. The described gyrotron tube has a cavity radius of 3 mm. Under normal operation, the accelerating voltage is 10 kV and the beam current is 50 mA, resulting in 20 W of microwave power at the fundamental modes. Several hundred of milliwatts are observed when operating at the second harmonic. The authors emphasize and discuss the mode competition problem.

High order axial (longitudinal) mode excitation by changing the magnetic field is a proven technique for obtaining wide range frequency tuning capabilities [48]. By using high order modes, smooth change is observed, as the characteristic values of the following $TE_{m,n,k}$ modes, where k is changing, are closely spaced. This implies that the cavity is relatively long, and that the middle part of the resonator is sometimes slightly up-tapered. A series of gyrotrons, which possess continuous tuning capability, have been demonstrated by several groups: MIT group gyrotrons, which use this technique described in [40, 42, 44, 49, 50]; Fukui group gyrotrons – described in [41,51–53]; CRPP-EPFL in Switzerland – described in [54–57]; KIT in Germany – described in [58,59]; and Nizhny Novgorod Technical University/GYCOM in Russia – described in [60–62].

In paper [49], continuous frequency tuning in the range of 2 GHz at the first harmonic frequency of 247 GHz is reported. Change is done by magnetic field variation in the range of $\langle 8.5 - 9.4 \rangle$ T. The authors focus their analysis on the smooth transition between high order axial modes. Linear theory, "MAGY" code and experimental results are compared for mode $TE_{5,2,k}$. The authors conclude that cavity design is crucial for a smooth transition between neighboring modes, and that this is where more work has to be done.

The gyrotron FU CW II is designed to work at a frequency of 394.6 GHz (second harmonic) with a power of 32 W. This satisfies the conditions of 600 MHz DNP-proton NMR [51]. An extra three coils installed in the gun region for optimal beam guidance allows the main magnet to be tuned from 4–8 T. At the gyrotron, an output high pass filter with a thin circular waveguide (diameter is 0.7 mm) was installed to sharpen the spectral lines of the RF field. On the other hand, the gyrotron FU CW III is designed to work at the second harmonic 1 THz frequency, with a wide tuning range from the sub-THz up to the THz region. Wide tunability can be achieved by changing the magnetic field of the main magnet, which implies working at different modes. A difficulty to overcome when producing 30 W

of power at a frequency of 1 THz is that a 20 T magnet and a 30 kV, 1 A beam power supply has to be used.

Most of the frequency tunable gyrotrons have relatively long cavities in order to provide a small frequency difference between the axial modes of the cavity, which is in order to obtain smooth frequency tuning. The drawback of this design is that radiation power decreases with an increasing axial index of the operating mode as a consequence of the electron velocity spread. In turn, the shortening of the cavity below the length that is optimal for the highest efficiency reduces the influence of the velocity spread, because de-bunching caused by the spread is not large over a short transit time. A shorter cavity requires a higher electron beam current in order to provide starting conditions for high order modes. By reducing the cavity length and the order of the operating transverse mode, a fairly wide frequency band of the gyrotron generation can be achieved [62]. In the paper, changes in output power and frequency caused by magnetic field variation is presented for the 0.2 THz gyrotron. The authors consider the theory of the influence of velocity spread on the output power and frequency in the short cavity gyrotron.

The smooth frequency tunable gyrotron in the gyro-BWO state is verified experimentally in the range of $\langle 134-140\rangle$ GHz, $TE_{0,6,k}$ mode, and in simulation $\langle 394-399\rangle$ GHz, $TE_{1,2,k}$ mode [63]. A scaled experiment was performed using the FU IV gyrotron. The authors proved a concept where the backward-wave component interacts with the electron beam. An electronic feedback loop is observed between the two, which in turn allows osculation to be smoothly tuned over a broad range. The electronic feedback loop also has a positive impact on the frequency stability, which is discussed further in another chapter in this article. The scaled experiment became the FU CW VI gyrotron, which is suitable for 600 MHz DNP-NMR [41]. It obtained a smooth tuning range of $\langle 394.65-396.27\rangle$ GHz of 1.6 GHz with output power of 10 W. The authors conclude that power stabilization by feedback control of the beam current is required under magnetic field change. For this reason the maximum output power was limited to 10 W in order for it to be stabilized in the whole frequency variation range.

In the comprehensive paper [40], on the 460 GHz MIT gyrotron redesigned for the DNP-NMR experiment important aspects are described. Furthermore, experimental data show that the gyrotron is able to generate 16 W of output power at the second harmonic with smooth frequency tunability of 1 GHz, which is around 20 times broader than for a typical submillimeter wave gyrotron. In this paper, the authors also discuss long-term stability.

4.3. Variation of cavity dimensions – the frequency tuning method

The effect of the frequency change with cavity temperature is reported in [64] to be $\sim 1\ \frac{\text{MHz}}{^\circ\text{C}}$. Another group reports a value of the $\sim 2\ \frac{\text{MHz}}{^\circ\text{C}}$ [65]. Temperature variation causes a change of cavity dimensions Fig. 4. When the equilibrium point is reached, it is not considered to negatively impact short-term stability. A tunable gyrotron is designed to change the operating mode, and in this case the effect of the temperature variation has to be taken into account, as together with the operating mode, output power may vary significantly and as a consequence it takes time to reach the new cavity temperature equilibrium. Another application case is when long-term (few days) stability is expected, which is the case with DNP-NMR. This method is not very common, but could be used for fine frequency tuning or compensation of changes caused by a variation of output power (when switching to a different operating mode). The advantage of this approach is that if the gyrotron has a build in cavity cooler, then the existing circuit can be used by controlling the coolant temperature [65].

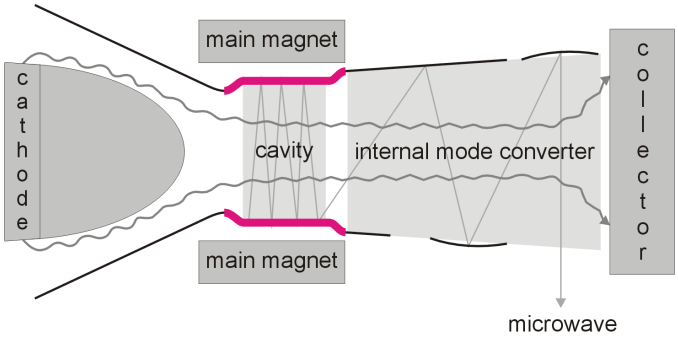

Fig. 4. Variation of the cavity dimensions mechanism. Cavity wall marked in color is moved, misaligned, stretched, squeezed for controlling frequency

In paper [66], interesting concepts are presented. The first is the use of so-called smart cavities, which actually means using material that has one or more properties that can be controlled by external stimulation. This kind of material is piezoelectric ceramic (e.g. Lead Zirconate Titanate PZT). The idea is to change the shape or dimension of the cavity during operation, together with the fine tuning of other parameters (magnetic field, beam current, voltage, pitch factor). Either one or more parts of the gyrotron could be made with piezoelectric material. Moreover, linear motors or actuators could be made with piezoelectric material in order to move other parts inside the gyrotron tube. The second concept is to use a cavity with disturbed axial symmetry (an ellipse) by squeezing the cavity that is made of elastic material. The authors discuss the theoretical background of the computer codes required to analyze such a case, and also present the numerical results.

4.4. Movable internal insert – the frequency tuning method

The theoretical background for the inner conductor concept is discussed in [67]. The concept of the movable, coaxial insert (Fig. 5) is numerically investigated in paper [68]. The authors almost achieved a 1 GHz tuning range in the 140 GHz 1.5 MW plasma gyrotron. The main drawback of this approach is mechanical manufacturing and alignment. For DNP-NMR gyrotrons, in which the radius of the cavity decreases to 1 mm, it seems impossible to fabricate the inner conductor, and therefore this method may be applied to sub-THz gyrotrons. A similar approach can be applied to create a mode generator for the

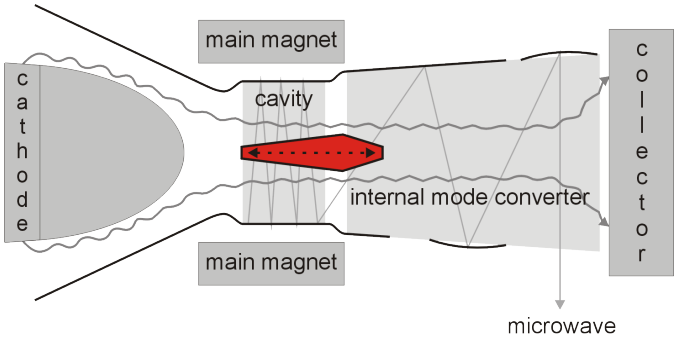

Fig. 5. Movable insert in the cavity region. Metal insert marked in color, placed inside gyrotron resonator is used for controlling frequency

so-called "cold testing" of gyrotron components. Resonant frequency and the quality factor are the same in the mode generator and gyrotron cavity. The main difference is that in the mode generator, mode selectivity by means of an electron beam does not exit. For this reason, other methods such as internal coaxial insert (with rod radius smaller than caustic radius R_c of generated mode), careful selection of the generation frequency or waveguide radius, smart geometry planning, have to be applied in order to enhance the designed mode and suppress competing ones. Such a prototype of a mode generator was reported in [69].

In paper [70], the concept of a coaxial cavity with smooth frequency tuning is tested numerically. A cone shaped rod is displaced by ± 1.5 mm along the gyrotron's longitudinal axis, which causes a smooth variation of the characteristic values of the cavity. The authors, in their results, report a 8 GHz tuning range at a 394.6 GHz central frequency with output power of several hundred watts.

4.5. Hysteresis-like effect in frequency tunable gyrotrons

One phenomenon worth mentioning is hysteresis (Fig. 6) with frequency tunability of the gyrotron [71, 72]. This effect is reported for both cathode voltage and magnetic field control. The observed dependence of the control value vs. output power is different when the control value is raised and when it is lowered (the plot creates a hysteresis loop). Actually, this is an effect that allows the tunability range to be broadened by the factor of $\Delta F_{\mathrm{mag}} = 2 \cdot 28 \cdot \Delta B/(1 + U/511)$ in the magnetic tuning, and $\Delta F_{\mathrm{volt}} = 2 \cdot 28 \cdot B/\Delta(1 + U/511)$ in the voltage tuning (in theory) [72]. In reality, this gain is smaller, as it is limited by frequency pulling.

4.6. Electron GUN heater voltage control – output power stability

In [64], the authors report that the output power is stable enough if the superconducting magnet drift is lower than 0.001 ppm/h. When short-therm stability is considered it can be assumed that output power is linearly proportional to the beam current. However in long-term perspective gyrotron parameters drift, which causes ouput power vs. beam current dependency to be not linear when long period of time is considered. Therefore beam current control is a sufficient method to stabilize output power only in the short-term perspective. For long-term operation, this method does not work well, because output power oscillates after a period of equilibration, and therefore the relation between beam current and power is not precise. The authors describe the methodology of finding the optimal PID (proportional, differential, derivative) regulator settings, however, the control value is the electron GUN heater voltage (Fig. 7), and not the beam current. The transient response of the Gyrotron for heater voltage control is presented. Voltage step up and step down (by 0.1 V) is applied, and then microwave diode power (gyrotron output power) is recorded over a time of 120 seconds. Temperature control has a relatively big inertia – around 58 second in this case. For this reason, a pure PID algorithm will fail to regulate. The authors add an additional routine to the PID algorithm. Measured data are input to the standard automotive Ziegler-Nichols PID tuning rule [73], however, the authors did not say what the initial pid settings were. It is unknown if the derivative part of the controller is turned off, as the D-part has a negative impact on the stability of the regulation algorithm for big inertia objects. Process data are filtered by a bandpass filter before they can be used as input for the control algorithm. Additionally, the PID controller on-line re-tuning is triggered every time a steady-state error exceeds the manually set threshold. The gyrotron's parameters drift over time, and PID theory assumes that a regulated object has constant parameters, therefore re-tuning is required. It is a well known limitation for this type of control, and better approach would probably be to implement a fuzzy logic controller [74], which is a common way to overcome this problem. However, there are many implementations of fuzzy controllers, so finding the optimal solution would require a lot of testing effort.

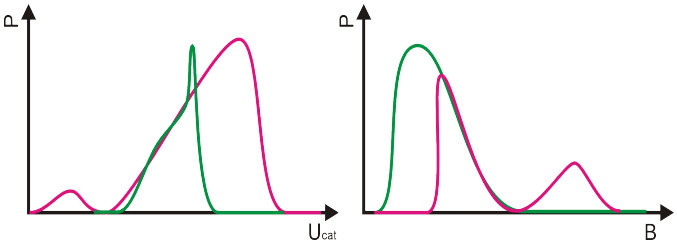

Fig. 6. Hysteresis loop. Cathode voltage, or magnetic field (red increasing, green decreasing) is changed to control frequency and power. Hysteresis behavior is observed, which can be exploited to extend tuning range slightly

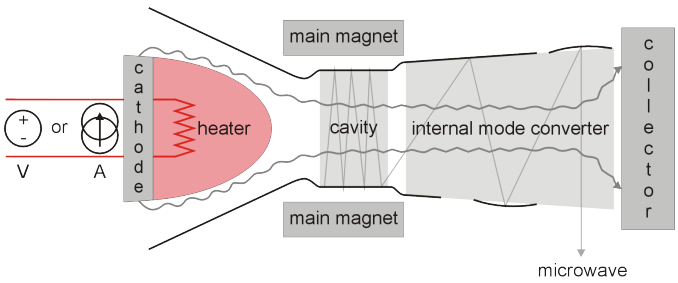

Fig. 7. Electron gun temperature control mechanism. Heater drawn in red is driven by current or voltage source. Change of the electron gun temperature is used for controlling electron beam current

4.7. Electron GUN heater current control – output power stability

In paper [38], the FU CW 394 GHz gyrotron for 600 MHz DNP-NMR optimization is reported. The authors applied a PID controller (by controlling the GUN heater current) to stabilize the electron beam current (Fig. 7). The heater temperature has a direct impact on the amount of electrons released from the GUN surface (beam current). This method was sufficient to stabilize the beam current, but not enough to obtain stable output power. The PID algorithm was too slow, when only controlling the heater's current, to suppresses rapid fluctuations. For this reason, another PID controller was applied. This approach is comprehensively described in paper [75], where three configurations are investigated. In the first configuration, the control value is the gun heater current, and the feedback (set point) value is the electron beam current. It is reported that one PID controller in this scheme reveals $\pm 6\%$ power fluctuations over 1 hour in the long term. Short-term disturbance is about $\pm 2.5\%$. The authors point out several reasons: fast fluctuations of power supply, mechanical shocks, the instrumental measuring noise of the diode, the amplifier, the digital to analog converter. In the second configuration, the control value is also the gun heater current, but the feedback (set point) value is the output power of the gyrotron (the same approach as in [38]). The authors report $\pm 1.8\%$ power stability, but an increasing PI coefficient for improving stabilization causes overshooting after several hours of normal operation. For this reason, PID was supplemented with an algorithm that reduces controller gain when high fluctuations are detected, and increases gain when small fluctuations are detected. This hybrid approach results in $\pm 0.7\%$ power stability over 6 hours of testing. The third configuration consists of two PID controllers. The first controller is the one from the first configuration, which stabilizes the electron beam current by controlling the gun heater current. The second controller uses output power as the feedback signal, and anode voltage as the control value. In this way, both the beam current and output power are stabilized. The response of the gun heater has high inertia, while the anode voltage control has an almost instant response. The advantage of the double PID is power deviation of $\pm 0.1\%$ as a result of the fast response of the anode voltage control. This proves that the PID algorithm can be applied for long-term gyrotron stabilization, but it requires some additional treatments.

4.8. The most important sources of frequency instability

The principle of a gyrotron's operation implies several sources of frequency instability. Electrons are emitted from the gun's surface, which is a statistical process. Electrons are accelerated by the cathode electric field and guided by the magnetic field. Each single electron path in the EM field is slightly different, which causes electron parameter spread. This fact is taken into account in the gyrotron equations as pitch factor and electron velocity spread. Additionally disturbing EM or mechanical agents appear. All these factors are the cause of long-therm and short-therm (rapidly changing) instabilities. The most important factors when considering gyrotron stability are cathode power supply and magnetic field stability. If any of those two is unstable considering other factors is useless. A more detailed description of all these difficulties is provided below:

- magnetic field inhomogeneity and stability – this is the first of two most important factors. The magnetic field has an impact on the electrons trajectory, and it determines the coupling efficiency factor. In the gyrotron system of equations, the parameters that describe these quantities are compression ratio α and cyclotron frequency ω_{cyc}.
- accelerating electric field – this is the second of two most important factors. The main cause of this instability is power supply voltage fluctuations. It determines the electron's initial kinetic energy, which is square related to the electron's velocity. In the gyrotron equations it will influence pitch factor $alpha$ and cyclotron frequency ω_{cyc}, and thus change the output power and frequency.
- mode competition – may cause the emission of two modes simultaneously, which is undesired for spectroscopy and may cause output power oscillations while two standing waves (modes) compete to gain energy. Both modes will influence the electrons path as the electric field superposition rule applies in this case.
- electron parameter spread – is mainly caused by the gun's emission surface, which cannot be infinitely thin. Each electron will have a different starting position against the electric and magnetic (guiding) field, and therefore trajectory and electron parameters will slightly differ within a certain range of values [76]. Electrons will have velocity and trajectory spectrum, and therefore released cyclotron energy will by divided among several frequencies [77]. Other factors can be described in general as EM field related [78,79]. To diagnose these problems, the axial velocity of electrons can be evaluated by analysis propagation of the gigahertz frequency signal in a slow-wave structure coupled with an electron beam [80].
- influence of self inductance – this is an important factor in megawatt gyrotrons (high electron current) and is usually neglected in low power devices, such as NMR gyrotrons. However, this effect is always present. It is observed when the electron's longitudinal speed is relatively low. A moving particle creates a magnetic field and disturbs the EM field in the resonator. The same particle is influenced by the disturbed magnetic field. In this way, the electron beam has an influence on itself. This situation may be especially evident when cathode (accelerating) voltage is low. In the gyrotron equations, this situation is determined by the comparing E field decay time with electron transition through the cavity time $t_{\mathrm{decay}} \gg t_{\mathrm{transit}}$, where $t_{\mathrm{decay}} \sim \frac{Q}{\omega}$ and $t_{\mathrm{transit}} \sim \frac{L}{V_z}$. Q – resonator quality factor, ω – E field angular frequency, L – resonator length, V_z – electron longitudinal velocity.
- Electrons can be disturbed by any unwanted EM field that will either travel back through the cavity's input taper, or will be created by the electrons trapped between the gun space and magnetic mirror [81].

Methods of stabilizing frequency can be divided into groups [82]:

- cathode voltage control,

- anode voltage control,
- magnetic field control,
- passive methods.

Gyrotrons employing these methods will be discussed.

4.9. Cathode voltage control – frequency stabilization

Initial electron kinetic energy is defined by the accelerating voltage. As a consequence, cyclotron frequency can by varied. This relation is described by equation [83]:

$$f_c \approx 28nB(1 - V_c/511), \tag{6}$$

where n – harmonic number, V_c – accelerating voltage kV, B – magnetic field T.

In paper [83], the authors report the frequency stability of the free-running gyrotron ≈ 10 MHz. After applying PID stabilization, 10 hours of operation revealed a frequency deviation of 0.6 MHz. Control voltage was applied between the cavity (body) and collector (ground potential). The high capacitance of the gyrotron body (ground), means that this method has a significantly lower PID bandwidth (fast variations of voltage are very difficult to achieve) [84] when compared to the anode voltage tuning method [62]. On the other hand, it does not require the high voltage cathode power supply to be modified. Every gyrotron that is built with a frequency tuning capability based on the accelerating voltage method can also be stabilized by the same means.

In [85], the authors discuss simultaneous stabilization of the output power and frequency. Intermediate frequency is measured and passed over as the feedback signal (PID input) for the PID controller, which in turn controls the voltage (PID output) of the gyrotron cavity (body). Therefore, the cathode voltage is varied to correct the cyclotron frequency. At the same time, the output power is measured by the RF diode and a proportional signal is applied to the anode voltage. By varying the anode voltage, the pitch factor is changed, and as a consequence the output power is controlled. Additionally, another PID controller is applied to control the electron gun heater current in order to extend power stabilization capabilities. All three PID controllers are implemented in LabView software in a digital manner. It is therefore natural to think that it is possible to combine the two input and three output signals by employing a more sophisticated algorithm and replacing the separate PID regulators in order to achieve much better stabilization. The authors report power stability of ±1% and frequency stability of ±1 MHz during 3 hours of testing, which is a little bit worse when compared to just the stabilization of frequency. However, for DNP-NMR, both output parameters are important, and therefore simultaneous stabilization is more advantageous.

Paper [86] describes frequency stabilization during power tuning at the same time as utilizing the relationship between the cathode voltage and pitch factor. In a typical gyrotron, variation of the cathode voltage has an impact on the operation frequency and output power. By stabilizing one value, the other is being changed at the same time. Contrary to the conventional feedback loop (wavenumber $k_z > 0$), in this case the gyrotron is working in the gyro-BWO (wavenumber $k_z < 0$) state at the first harmonic $TE_{12,2}$ mode. The magnetic field is constant and selected in order to match the desired RF frequency. The operation mechanism is different, as it results from compensation of detuning the electron cyclotron frequency during electronic tuning. This phenomena is described by two equations:

$$\omega \approx k_z V_z + s\Omega_e = k_z c\sqrt{\left(\frac{1-1/\gamma^2}{1+\alpha^2}\right)} + \frac{seB}{m_e\gamma}, \tag{7}$$

$$\gamma = 1 + \frac{eV}{m_e c^2}. \tag{8}$$

V is positively related to γ, and therefore an increase of voltage V leads to a decrease of electron cyclotron frequency Ω_e. If pitch factor α gets larger at the same time, the decrease of the absolute value of Doppler shift $k_z V_z$ can compensate the decrease of Ω_e in the gyro-BWO state ($k_z < 0$!). As a result, operating frequency ω will remain unchanged. The authors investigate this idea of a low-voltage cathode, and as a result: for V change by 0.796 kV and α by 0.8 – the frequency changes by 6.3 MHz. For high voltage operation, V change is 1.61 kV and α is 0.8 – the frequency difference is 13.5 MHz. In conventional cases ($k_z > 0$) reported in the literature, a typical change of frequency is 50 MHz/kV. An essential point reported in this paper is that together with pitch factor variation, output power is smoothly tuned by 40%. The authors dedicate this solution to high power THz heating in material science and bio-medicine (the stability is not satisfactory for NMR). However, the electronic detuning concept might be promising when applied to NMR low voltage gyrotrons.

4.10. Anode voltage control – frequency stabilization

The main advantage of this method is that it is independent from the cathode and body potential. It combines low voltage, low current operation and low capacitance. Technically it can be achieved by employing triode gun design [87–89] or by separating the potential of anode + cavity from a collector part of the gyrotron as it is proposed in the extremely well illustrated work [90]. There are several technical variations, but the same principle. Described control system has an increased bandwidth,

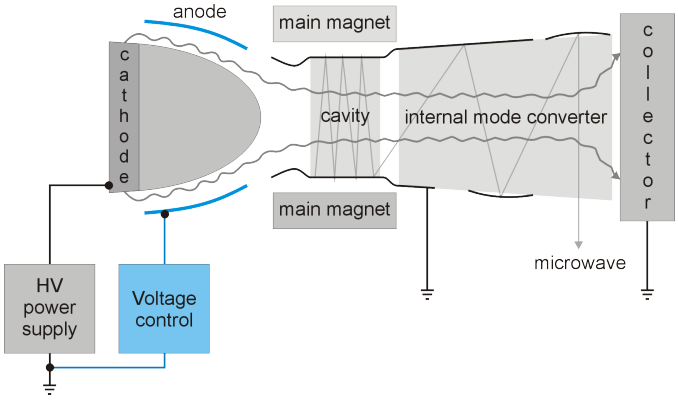

Fig. 8. Anode voltage control mechanism. Anode and additional power supply marked in color are used to change voltage between cathode and anode. Low capacity of the anode allows high control bandwidth

while keeping the same frequency sensitivity when compared to the cathode voltage method. In this approach, the pitch factor of the electrons is varied. In paper [82], the 263 GHz 1 kW GYCOM gyrotron is tested. An anode control voltage variation of 1 kV and a speed better than 1 $\frac{\text{kV}}{\mu\text{s}}$ is delivered by a separate power supply, so no intrusion in the main power supply is required. Frequency sensitivity of 33 MHz/kV is obtained in both the experiment and the theory. In paper [91], the same GYCOM 263 GHz 1 kW gyrotron is presented, however, the article focuses on comparing the theoretical calculations and experimental data. The frequency pulling effect is explained and simulation difficulty is outlined. The theoretical and experimental dependence of frequency shift (0–40 MHz) vs. anode voltage variation (0–1 kV) is compared. In the theoretical study, it is concluded that the optimal spectroscopic regime is not in the highest efficiency working point, but in the middle of the generation zone. Sensitivity of the anode voltage frequency tuning varies from 5 to 30 MHz/kV, which is in accordance with the theoretical calculations and depends on the gyrotrons working point (magnetic field). The reported theory and experiment discrepancy is smaller than 3×10^{-5}, which proves the credibility of the approach presented in [91]. The total frequency tuning range was 4 MHz with frequency stability of 1 Hz, which can be compared to a stability of 0.5 MHz for the free running gyrotron [62].

4.11. Passive stabilization – frequency stabilization

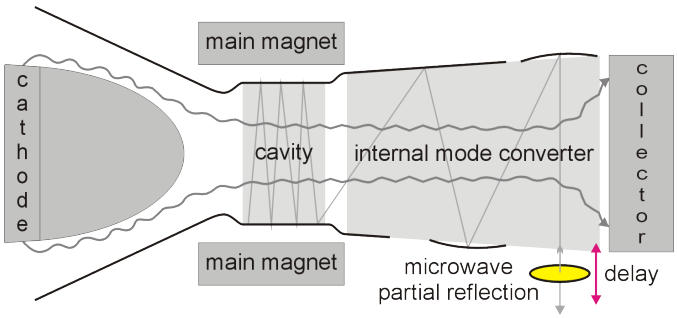

Fig. 9. Passive stabilization by delayed reflected beam self-injection. Small part of the microwave beam is reflected back to the cavity. Reflector is placed outside the gyrotron tube

Frequency stabilization by delayed reflection of the output radiation is experimentally simple as it is done outside the gyrotron tube [62]. Experimental and theoretical results were reported in [92]. The authors conclude that for a large delay time (long distance 3.5 m) between the gyrotron output and reflector (e.g. Teflon disk), even a few percent of reflection of the microwave power results in an increase of the gyrotron's stability by a factor of 2, while in theory the maximal increase can be 3 times [62].

In paper [93], a high-resonant and non-resonant load, as a reflector is considered numerically. The authors derive a self-consistent equation with load included, and then conclude the conditions of optimal operation for both cases. Resonant frequency with and without load reveals hysteresis behavior when changed, and thus the reflected wave can hold gyrotron frequency within a narrow band. The authors of paper [94] verified the theory experimentally, and also with the use of the particle in cell simulation method. The bandwidth of the free-running gyrotron was ~ 3.1 MHz, while its setup with reflections and phase correctly aligned had a bandwidth ~ 1.9 MHz, causing stability to be better by a factor of 1.6.

In paper [95], a theoretical study of a self-consistent, time domain equation is presented. Boundary conditions are changed to match the case when gyrotron output is connected to the resonant load (external resonator). The authors discuss the impact on the EM field profile inside the interaction space. The reported boundary conditions can be used for materials with a reflection coefficient defined as a function of frequency.

One more theoretical study [96] reveals the influence of delayed reflection on frequency tuning by a magnetic field, while the same author [97] also theoretically investigated the possibility of controlling mode competition by adjusting the reflection coefficient. In some cases, parasitic modes can be suppressed by proper phase matching of the reflected, self-injected wave. This might be interesting and useful, especially in high frequency gyrotrons with smooth tuning capabilities, where mode competition is an important problem. Thus, these modes have similar starting conditions.

4.12. Double beam gyrotrons – demand for high frequency

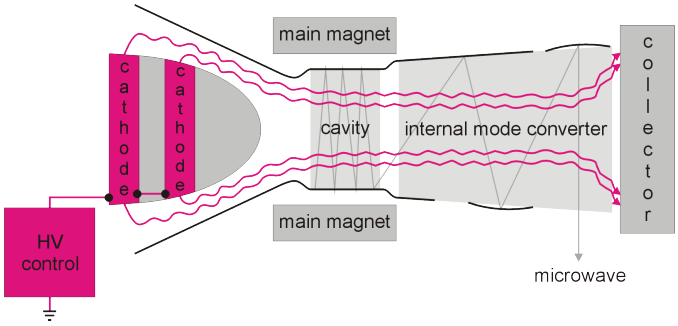

Fig. 10. Double beam gyrotron mechanism. Two cathode strips marked in color are required to generate two beams. One beam is aligned to enhance the desired mode, second beam is used to suppress the parasitic modes

To achieve high frequency generation, second and third harmonic operation has to be employed. Mode competition becomes very difficult to overcome due to the fact that characteristic values of neighbouring modes are similar at high harmonic operation. The proposed 780 GHz gyrotron operates at the second harmonic with output power of 10 W. It is designed to generate two electron beams [98]. In such a construction, the beam radius of each beam is chosen in such a way that the first beam feeds the desired RF field mode, and the second beam consumes energy from the RF field to suppress parasitic modes. In this manner, mode selectivity is achieved. The authors are developing a third harmonic gyrotron to operate at a record 1.2 THz frequency. This device requires a double beam design, but its small cavity radius of 2.5 mm makes it difficult to position and

to generate a suppressing beam. Moreover, manufacturing accuracy of 0.01λ becomes a limiting factor. The authors claim that the use of multi-beam gyrotrons is now the most promising method to increase operating frequency in the terahertz range.

In paper [99], a double beam, low voltage gyrotron is reported, and a three electrode magnetron injection gun is employed. The authors examine the magnetic field values in the range of 11.06 to 14.95 T. The gyrotron was designed for second harmonic operation at an accelerating voltage of 20 kV, however, the authors lowered it to 2.4 kV – 5 kV and reported first harmonic operation. Further optimization of the electron beam's parameters was done by varying the anode voltage (Fig. 8) in the range from 0 to –1 kV. It was revealed that at cathode voltages lower than 5 kV, the recorded frequency was 460 GHz and the power level obtained was 60 W, which is satisfying for DNP-NMR spectroscopy.

5. CONCLUSIONS

The gyrotron is the only sensible source of high power microwave radiation for NMR enhanced experiments and power demanding terahertz applications [100]. On the other hand, semiconductor sources are not available for this power and frequency. With a proper control algorithm it surpasses other vacuum sources in terms of cost, life time and operating parameters [101]. The gyrotron can provide 0.5 MHz frequency and $\pm 0.1\%$ long-term power stability when it is supplied with the stabilization algorithm, which is a hybrid solution of PID control and the expert system. It can provide a power level of 10–100 W in a frequency range up to 1 THz.

There is no better microwave source for DNP-NMR experiments available at the present time.

REFERENCES

[1] H. Gunther, *NMR Spectroscopy: Basic Principles, Concepts and Applications in Chemistry*. Wiley, 2013.

[2] K. Zia, T. Siddiqui, S. Ali, I. Farooq, M. S. Zafar, and Z. Khurshid, "Nuclear Magnetic Resonance Spectroscopy for Medical and Dental Applications: A Comprehensive Review," *Eur. J. Dentistry*, vol. 13, no. 01, pp. 124–128, Feb. 2019, doi: 10.1055/s-0039-1688654.

[3] R.A. de Graaf, *In Vivo NMR Spectroscopy: Principles and Techniques*. John Wiley and Sons Ltd., 2019, doi: 10.1002/9781119382461.

[4] M.E. Smith and J.H. Strange, "NMR techniques in materials physics: a review," *Meas. Sci. Technol.*, vol. 7, no. 4, pp. 449–475, Apr. 1996, doi: 10.1088/0957-0233/7/4/002.

[5] V.S. Mandala and M. Hong, "High-sensitivity protein solid-state NMR spectroscopy," *Curr. Opin. Struct. Biol.*, vol. 58, pp. 183–190, Oct. 2019, doi: 10.1016/j.sbi.2019.03.027.

[6] K. Inomata *et al.*, "High-resolution multi-dimensional NMR spectroscopy of proteins in human cells," *Nature*, vol. 458, no. 7234, pp. 106–109, Mar. 2009, doi: 10.1038/nature07839.

[7] E. Hatzakis, "Nuclear Magnetic Resonance (NMR) Spectroscopy in Food Science: A Comprehensive Review: NMR spectroscopy in food science," *Compr. Rev. Food Sci. Food Saf.*, vol. 18, no. 1, pp. 189–220, Jan. 2019, doi: 10.1111/1541-4337.12408.

[8] P.H. Keizers *et al.*, "Benchtop NMR spectroscopy in the analysis of substandard and falsified medicines as well as illegal drugs," *J. Pharm. Biomed. Anal.*, vol. 178, p. 112939, Jan. 2020, doi: 10.1016/j.jpba.2019.112939.

[9] A.W. Chan *et al.*, "1H-NMR urinary metabolomic profiling for diagnosis of gastric cancer," *Br. J. Cancer*, vol. 114, no. 1, pp. 59–62, Jan. 2016, doi: 10.1038/bjc.2015.414.

[10] J.K. Nicholson, I.D. Wilson, and J.C. Lindon, "Pharmacometabonomics as an effector for personalized medicine," *Pharmacogenomics*, vol. 12, no. 1, pp. 103–111, Jan. 2011, doi: 10.2217/pgs.10.157.

[11] D. Chen, Z. Wang, D. Guo, V. Orekhov, and X. Qu, "Review and Prospect: Deep Learning in Nuclear Magnetic Resonance Spectroscopy," *Chem.-Eur. J.*, p. chem.202000246, Jun. 2020, doi: 10.1002/chem.202000246.

[12] D. Svozil, V. Kvasnicka, and J. Pospichal, "Introduction to multi-layer feed-forward neural networks," *Chemometrics Intell. Lab. Syst.*, vol. 39, no. 1, pp. 43–62, Nov. 1997, doi: 10.1016/S0169-7439(97)00061-0.

[13] N. Aloysius and M. Geetha, "A review on deep convolutional neural networks," in *2017 International Conference on Communication and Signal Processing (ICCSP)*. Chennai: IEEE, Apr. 2017, pp. 0588–0592, doi: 10.1109/ICCSP.2017.8286426.

[14] A. Krizhevsky, I. Sutskever, and G.E. Hinton, "ImageNet classification with deep convolutional neural networks," *Commun. ACM*, vol. 60, no. 6, pp. 84–90, May 2017, doi: 10.1145/3065386.

[15] R.J. Williams and D. Zipser, "A learning algorithm for continually running fully recurrent neural networks," *Neural Comput.*, vol. 1, no. 2, pp. 270–280, 1989, doi: 10.1162/neco.1989.1.2.270.

[16] G.S. Nusinovich, M.K.A. Thumm, and M.I. Petelin, "The Gyrotron at 50: Historical Overview," *J. Infrared Millim. Terahertz Waves*, vol. 35, no. 4, pp. 325–381, Apr. 2014, doi: 10.1007/s10762-014-0050-7.

[17] E. Plinski, "Gorky's Gyrotron Heroes," *Bull. Pol. Acad. Sci. Tech. Sci.*, vol. 68, no. 6, pp. 1257–1262, 2020, doi: 10.24425/bpasts.2020.135392.

[18] M. Thumm, "State-of-the-Art of High-Power Gyro-Devices and Free Electron Masers," *J. Infrared Millim. Terahertz Waves*, vol. 41, no. 1, pp. 1–140, Jan. 2020, doi: 10.1007/s10762-019-00631-y.

[19] R. Temkin, V. Granatstein, and G.S. Nusinowich, *Introduction to the Physics of Gyrotrons*. Johns Hopkins University Press, 2004, doi: 10.1353/book.62236.

[20] V. Bargmann, L. Michel, and V.L. Telegdi, "Precession of the Polarization of Particles Moving in a Homogeneous Electromagnetic Field," *Phys. Rev. Lett.*, vol. 2, no. 10, pp. 435–436, May 1959, doi: 10.1103/PhysRevLett.2.435.

[21] B. Plainchont, P. Berruyer, J.-N. Dumez, S. Jannin, and P. Giraudeau, "Dynamic Nuclear Polarization Opens New Perspectives for NMR Spectroscopy in Analytical Chemistry," *Anal. Chem.*, vol. 90, no. 6, pp. 3639–3650, Mar. 2018, doi: 10.1021/acs.analchem.7b05236.

[22] A.W. Overhauser, "Polarization of Nuclei in Metals," *Phys. Rev.*, vol. 92, no. 2, pp. 411–415, Oct. 1953, doi: 10.1103/PhysRev.92.411.

[23] S. Pylaeva, K.L. Ivanov, M. Baldus, D. Sebastiani, and H. Elgabarty, "Molecular Mechanism of Overhauser Dynamic Nuclear Polarization in Insulating Solids," *J. Phys. Chem. Lett.*, vol. 8, no. 10, pp. 2137–2142, May 2017, doi: 10.1021/acs.jpclett.7b00561.

[24] H. Heise and S. Matthews, *Modern NMR Methodology*. Springer, Berlin, Heidelberg, 2013, doi: 10.1007/978-3-642-37991-8.

[25] M.L. Mak-Jurkauskas and R.G. Griffin, "High-Frequency Dynamic Nuclear Polarization," in *Encyclopedia of Magnetic Resonance*, R.K. Harris, Ed. Chichester, UK: John Wiley & Sons, Ltd, Mar. 2010, doi: 10.1002/9780470034590.emrstm1183.

[26] L. Thankamony, S. Aany, J.J. Wittmann, M. Kaushik, and B. Corzilius, "Dynamic nuclear polarization for sensitivity enhancement in modern solid-state NMR," *Prog. Nucl. Magn. Reson. Spectrosc.*, vol. 102-103, pp. 120–195, Nov. 2017, doi: 10.1016/j.pnmrs.2017.06.002.

[27] E.A. Nanni, A.B. Barnes, R.G. Griffin, and R.J. Temkin, "THz Dynamic Nuclear Polarization NMR," *IEEE Trans. Terahertz Sci. Technol.*, vol. 1, no. 1, pp. 145–163, Sep. 2011, doi: 10.1109/TTHZ.2011.2159546.

[28] M. Pourfathi *et al.*, "Low-temperature dynamic nuclear polarization of gases in Frozen mixtures: Method for DNP of Gases in Frozen Mixtures," *Magn. Reson. Med.*, vol. 76, no. 3, pp. 1007–1014, Sep. 2016, doi: 10.1002/mrm.26002.

[29] K.V. Kovtunov *et al.*, "Hyperpolarized NMR Spectroscopy: *d*-DNP, PHIP, and SABRE Techniques," *Chem. Asian J.*, vol. 13, no. 15, pp. 1857–1871, Aug. 2018, doi: 10.1002/asia.201800551.

[30] G. Pavlovskaya, J. Six, T. Meersman, N. Gopinathan, and S.P. Rigby, "NMR imaging of low pressure, gas-phase transport in packed beds using hyperpolarized xenon-129," *AlChE J.*, vol. 61, no. 11, pp. 4013–4019, Nov. 2015, doi: 10.1002/aic.14929.

[31] M. Ha and V.K. Michaelis, "High-frequency dynamic nuclear polarization nmr for solids: Part 1 – an introduction," in *Modern Magnetic Resonance*, G.A. Webb, Ed. Cham: Springer International Publishing, 2017, pp. 1–24, doi: 10.1007/978-3-319-28275-6_140-1.

[32] K.J. Pike *et al.*, "A spectrometer designed for 6.7 and 14.1T DNP-enhanced solid-state MAS NMR using quasi-optical microwave transmission," *J. Magn. Reson.*, vol. 215, pp. 1–9, Feb. 2012, doi: 10.1016/j.jmr.2011.12.006.

[33] Y. Matsuki *et al.*, "Helium-cooling and -spinning dynamic nuclear polarization for sensitivity-enhanced solid-state NMR at 14T and 30K," *J. Magn. Reson.*, vol. 225, pp. 1–9, Dec. 2012, doi: 10.1016/j.jmr.2012.09.008.

[34] K.R. Chu, "The electron cyclotron maser," *Rev. Mod. Phys.*, vol. 76, no. 2, p. 52, 2004.

[35] T. Idehara, Y. Shimizu, I. Ogawa, T. Tatsukawa, and G.F. Brand, "Rapid frequency step-switching in submillimeter wave gyrotrons (Gyrotrons FU III and FU IV)," *Phys. Plasma*, vol. 6, no. 6, pp. 2613–2617, Jun. 1999, doi: 10.1063/1.873533.

[36] T. Idehara, M. Pereyaslavets, N. Nishida, K. Yoshida, and I. Ogawa, "Frequency Modulation in a Submillimeter-Wave Gyrotron," *Phys. Rev. Lett.*, vol. 81, no. 9, pp. 1973–1976, Aug. 1998, doi: 10.1103/PhysRevLett.81.1973.

[37] T. Idehara *et al.*, "High speed frequency modulation of a 460 GHz gyrotron for application to the 700 MHz DNP enhanced NMR spectroscopy," in *2015 40th International Conference on Infrared, Millimeter, and Terahertz waves (IRMMW-THz)*. Hong Kong, China: IEEE, Aug. 2015, pp. 1–2, doi: 10.1109/IRMMW-THz.2015.7327859.

[38] K. Ueda, Y. Matsuki, T. Fujiwara, Y. Tatematsu, I. Ogawa, and T. Idehara, "Further Characterization of 394-GHz Gyrotron FU CW GII with Additional PID Control System for 600-MHz DNP-SSNMR Spectroscopy," *J. Infrared Millim. Terahertz Waves*, vol. 37, no. 9, pp. 825–836, Sep. 2016, doi: 10.1007/s10762-016-0276-7.

[39] L. Luo, S. Pan, C.-H. Du, M.-G. Huang, and P.-K. Liu, "Terahertz Ultralow-Voltage Gyrotron With Upstream Output," *IEEE Trans. Plasma Sci.*, vol. 48, no. 4, pp. 1195–1201, Apr. 2020, doi: 10.1109/TPS.2020.2979224.

[40] A.C. Torrezan *et al.*, "Continuous-Wave Operation of a Frequency-Tunable 460-GHz Second-Harmonic Gyrotron for Enhanced Nuclear Magnetic Resonance," *IEEE Trans. Plasma Sci.*, vol. 38, no. 6, pp. 1150–1159, Jun. 2010, doi: 10.1109/TPS.2010.2046617.

[41] T. Idehara *et al.*, "Continuously Frequency Tunable High Power Sub-THz Radiation Source–Gyrotron FU CW VI for 600 MHz DNP-NMR Spectroscopy," *J. Infrared Millim. Terahertz Waves*, vol. 31, no. 7, pp. 775–790, Jul. 2010, doi: 10.1007/s10762-010-9643-y.

[42] A.B. Barnes, E.A. Nanni, J. Herzfeld, R.G. Griffin, and R.J. Temkin, "A 250 GHz gyrotron with a 3 GHz tuning bandwidth for dynamic nuclear polarization," *J. Magn. Reson.*, vol. 221, pp. 147–153, Aug. 2012, doi: 10.1016/j.jmr.2012.03.014.

[43] T. Idehara *et al.*, "460 GHz second harmonic gyrotrons for a 700 MHz DNP-NMR spectroscopy," in *2013 38th International Conference on Infrared, Millimeter, and Terahertz Waves (IRMMW-THz)*. Mainz, Germany: IEEE, Sep. 2013, pp. 1–2, doi: 10.1109/IRMMW-THz.2013.6665482.

[44] S. Jawla *et al.*, "Continuously Tunable 250 GHz Gyrotron with a Double Disk Window for DNP-NMR Spectroscopy," *J. Infrared Millim. Terahertz Waves*, vol. 34, no. 1, pp. 42–52, Jan. 2013, doi: 10.1007/s10762-012-9947-1.

[45] R.K. Singh and M. Thottappan, "Design and PIC Simulation Studies of Millimeter-Wave-Tunable Gyrotron Using Metal PBG Cavity as its RF Interaction Circuit," *IEEE Trans. Plasma Sci.*, vol. 48, no. 4, pp. 845–851, Apr. 2020, doi: 10.1109/TPS.2020.2974791.

[46] W. Fu, X. Guan, and Y. Yan, "Generating High-Power Continuous-Frequency Tunable Sub-Terahertz Radiation From a Quasi-Optical Gyrotron With Confocal Waveguide," *IEEE Electron Device Lett.*, vol. 41, no. 4, pp. 613–616, Apr. 2020, doi: 10.1109/LED.2020.2972380.

[47] K.D. Hong, G.F. Brand, and T. Idehara, "A 150–600 GHz step-tunable gyrotron," *J. Appl. Phys.*, vol. 74, no. 8, pp. 5250–5258, Oct. 1993, doi: 10.1063/1.354265.

[48] S.P. Sabchevski and T. Idehara, "A numerical study on finite-bandwidth resonances of high-order axial modes (HOAM) in a gyrotron cavity," *J. Infrared Millim. Terahertz Waves*, vol. 36, no. 7, pp. 628–653, 2015.

[49] M. Hornstein *et al.*, "Second Harmonic Operation at 460 GHz and Broadband Continuous Frequency Tuning of a Gyrotron Oscillator," *IEEE Trans. Electron Devices*, vol. 52, no. 5, pp. 798–807, May 2005, doi: 10.1109/TED.2005.845818.

[50] R.J. Temkin, "Development of terahertz gyrotrons for spectroscopy at MIT," *THz Sci. Technol.*, vol. 7, no. 1, pp. 1–9, 2014.

[51] T. Idehara *et al.*, "The 1 THz gyrotron at Fukui University," in *2007 Joint 32nd International Conference on Infrared and Millimeter Waves and the 15th International Conference on Terahertz Electronics*. Cardiff: IEEE, Sep. 2007, pp. 309–311, doi: 10.1109/ICIMW.2007.4516512.

[52] V. Bratman *et al.*, "Review of Subterahertz and Terahertz Gyrodevices at IAP RAS and FIR FU," *IEEE Trans. Plasma Sci.*, vol. 37, no. 1, pp. 36–43, Jan. 2009, doi: 10.1109/TPS.2008.2004787.

[53] T. Idehara and S.P. Sabchevski, "Development and Applications of High–Frequency Gyrotrons in FIR FU Covering the sub-THz to THz Range," *J. Infrared Millim. Terahertz Waves*, vol. 33, no. 7, pp. 667–694, Jul. 2012, doi: 10.1007/s10762-011-9862-x.

[54] S. Alberti *et al.*, "Experimental study from linear to chaotic regimes on a terahertz-frequency gyrotron oscillator," *Phys. Plasma*, vol. 19, no. 12, p. 123102, Dec. 2012, doi: 10.1063/1.4769033.

[55] J.-P. Hogge *et al.*, "Detailed characterization of a frequency-tunable 260 GHz gyrotron oscillator planned for DNP/NMR spectroscopy," in *2013 38th International Conference on Infrared, Millimeter, and Terahertz Waves (IRMMW-THz)*. Mainz, Germany: IEEE, Sep. 2013, pp. 1–2, doi: 10.1109/IRMMW-THz.2013.6665407.

[56] Y. Rozier *et al.*, "Manufacturing of a 263 GHz continuously tunable gyrotron," in *2013 IEEE 14th International Vacuum Electronics Conference (IVEC)*. Paris, France: IEEE, May 2013, pp. 1–2, doi: 10.1109/IVEC.2013.6571071.

[57] F. Braunmueller, T.M. Tran, S. Alberti, J.-P. Hogge, and M.Q. Tran, "Moment-based, self-consistent linear analysis of gyrotron oscillators," *Phys. Plasma*, vol. 21, no. 4, p. 043105, Apr. 2014, doi: 10.1063/1.4870082.

[58] M. Thumm *et al.*, "Frequency step-tunable (114–170 GHz) megawatt gyrotrons for plasma phys., applications," *Fusion Eng. Des.*, vol. 53, no. 1-4, pp. 407–421, Jan. 2001, doi: 10.1016/S0920-3796(00)00519-6.

[59] E. Borie *et al.*, "Possibilities for multifrequency operation of a gyrotron at fzk," *IEEE Trans. Plasma Sci.*, vol. 30, no. 3, pp. 828–834, Jun. 2002, doi: 10.1109/TPS.2002.801561.

[60] V. Zapevalov *et al.*, "Optimization of the frequency step tunable 105–170 GHz 1 MW gyrotron prototype," in *Twenty Seventh International Conference on Infrared and Millimeter Waves*. San Diego, CA, USA: IEEE, 2002, pp. 1–2, doi: 10.1109/ICIMW.2002.1076054.

[61] M.Y. Glyavin *et al.*, "Experimental tests of a 263 GHz gyrotron for spectroscopic applications and diagnostics of various media," *Rev. Sci. Instrum.*, vol. 86, no. 5, p. 054705, May 2015, doi: 10.1063/1.4921322.

[62] G.G. Denisov, M.Y. Glyavin, A.E. Fedotov, and I.V. Zotova, "Theoretical and Experimental Investigations of Terahertz-Range Gyrotrons with Frequency and Spectrum Control," *J. Infrared Millim. Terahertz Waves*, vol. 41, pp. 1131–1143, Mar. 2020, doi: 10.1007/s10762-020-00672-8.

[63] T.H. Chang, T. Idehara, I. Ogawa, L. Agusu, and S. Kobayashi, "Frequency tunable gyrotron using backward-wave components," *J. Appl. Phys.*, vol. 105, no. 6, p. 063304, Mar. 2009, doi: 10.1063/1.3097334.

[64] V.S. Bajaj *et al.*, "250GHz CW gyrotron oscillator for dynamic nuclear polarization in biological solid state NMR," *J. Magn. Reson.*, vol. 189, no. 2, pp. 251–279, Dec. 2007, doi: 10.1016/j.jmr.2007.09.013.

[65] S.-T. Han *et al.*, "Spectral Characteristics of a 140-GHz Long-Pulsed Gyrotron," *IEEE Trans. Plasma Sci.*, vol. 35, no. 3, pp. 559–564, Jun. 2007, doi: 10.1109/TPS.2007.896931.

[66] S. Sabchevski and T. Idehara, "Resonant Cavities for Frequency Tunable Gyrotrons," *Int. J. Infrared Millimeter Waves*, vol. 29, no. 1, pp. 1–22, Jan. 2008, doi: 10.1007/s10762-007-9297-6.

[67] C.T. Iatrou, S. Kern, and A.B. Pavalyev, "Coaxial Cavities with Corrugated Inner Conductor for Gyrotrons," *IEEE Trans. Microwave Theory Tech.*, vol. 44, no. 1, pp. 56–64, 1996, doi: 10.1109/22.481385.

[68] O. Dumbrajs and A. Mobius, "Tunable coaxial gyrotron for plasma heating and diagnostics," *Int. J. Electron.*, vol. 84, no. 4, pp. 411–419, Apr. 1998, doi: 10.1080/002072198134751.

[69] M. Pereyaslavets, O. Braz, S. Kern, M. Losert, A. Mobius, and M. Thumm, "Improvements of mode converters for low-power excitation of gyrotron-type modes," *Int. J. Electron.*, vol. 82, no. 1, pp. 107–116, 1997, doi: 10.1080/002072197136291.

[70] M. Glyavin, V. Khizhnyak, A. Luchinin, T. Idehara, and T. Saito, "The Design of the 394.6 Ghz Continuously Tunable Coaxial Gyrotron for DNP Spectroscopy," *Int. J. Infrared Millimeter Waves*, vol. 29, no. 7, pp. 641–648, Jul. 2008, doi: 10.1007/s10762-008-9364-7.

[71] O. Dumbrajs, T. Idehara, Y. Iwata, S. Mitsudo, I. Ogawa, and B. Piosczyk, "Hysteresis-like effects in gyrotron oscillators," *Phys. Plasma*, vol. 10, no. 5, pp. 1183–1186, May 2003, doi: 10.1063/1.1561277.

[72] O. Dumbrajs, E.M. Khutorysn, and T. Idehara, "Hysteresis and frequency tunability of gyrotrons," in *2015 40th International Conference on Infrared, Millimeter, and Terahertz waves (IRMMW-THz)*. Hong Kong, China: IEEE, Aug. 2015, pp. 1–1, doi: 10.1109/IRMMW-THz.2015.7327858.

[73] M. Meshram, "Tuning of PID controller using Ziegler-Nichols method for speed control of DC motor," in *IEEE-International Conference On Advances In Engineering, Science And Management (ICAESM -2012)*, 2012, pp. 117–122.

[74] A. Noshadi, J. Shi, W.S. Lee, P. Shi, and A. Kalam, "Optimal PID-type fuzzy logic controller for a multi-input multi-output active magnetic bearing system," *Neural Comput. Appl.*, vol. 27, no. 7, p. 2031–2046, Oct 2016, doi: 10.1007/s00521-015-1996-7.

[75] E.M. Khutoryan, T. Idehara, A.N. Kuleshov, and K. Ueda, "Gyrotron Output Power Stabilization by PID Feedback Control of Heater Current and Anode Voltage," *J. Infrared Millim. Terahertz Waves*, vol. 35, no. 12, pp. 1018–1029, Dec. 2014, doi: 10.1007/s10762-014-0105-9.

[76] O.I. Louksha, D.B. Samsonov, G.G. Sominski, and S.V. Syomin, "Suppression of emission nonuniformity effect in gyrotrons," in *2014 39th International Conference on Infrared, Millimeter, and Terahertz waves (IRMMW-THz)*. Tucson, AZ, USA: IEEE, Sep. 2014, pp. 1–2, doi: 10.1109/IRMMW-THz.2014.6956492.

[77] O. Dumbrajs and T. Idehara, "Study of Mode Competition in the Third Harmonic Gyrotron with Inclusion of the Electron Velocity Spread and the Beam Width," in *2018 43rd International Conference on Infrared, Millimeter, and Terahertz Waves (IRMMW-THz)*. Nagoya: IEEE, Sep. 2018, pp. 1–2, doi: 10.1109/IRMMW-THz.2018.8509845.

[78] O. Louksha, B. Piosczyk, G. Sominski, M. Thumm, and D. Samsonov, "On potentials of gyrotron efficiency enhancement: measurements and simulations on a 4-mm gyrotron," *IEEE Trans. Plasma Sci.*, vol. 34, no. 3, pp. 502–511, Jun. 2006, doi: 10.1109/TPS.2006.875779.

[79] O.I. Louksha, D.B. Samsonov, G.G. Sominski, and S.V. Syomin, "Improvement of electron beam quality and gyrotron efficiency by optimization of electric field distribution in the gun region," in *2013 38th International Conference on Infrared, Millimeter, and Terahertz Waves (IRMMW-THz)*. Mainz, Germany: IEEE, Sep. 2013, pp. 1–2, doi: 10.1109/IRMMW-THz.2013.6665437.

[80] O.I. Louksha *et al.*, "Gyrotron Research at SPbPU: Diagnostics and Quality Improvement of Electron Beam," *IEEE Trans. Plasma Sci.*, vol. 44, no. 8, pp. 1310–1319, Aug. 2016, doi: 10.1109/TPS.2016.2590143.

[81] O.I. Louksha, "Numerical simulation of low-frequency collective processes in gyrotron electron beams," in *35th International Conference on Infrared, Millimeter, and Terahertz Waves*. Rome, Italy: IEEE, Sep. 2010, pp. 1–2, doi: 10.1109/ICIMW.2010.5613030.

[82] A. Fokin *et al.*, "High-power sub-terahertz source with a record frequency stability at up to 1 Hz," *Sci. Rep.*, vol. 8, no. 1, p. 4317, Dec. 2018, doi: 10.1038/s41598-018-22772-1.

[83] E.M. Khutoryan *et al.*, "Stabilization of Gyrotron Frequency by PID Feedback Control on the Acceleration Voltage," *J. Infrared Millim. Terahertz Waves*, vol. 36, no. 12, pp. 1157–1163, Dec. 2015, doi: 10.1007/s10762-015-0212-2.

[84] T. Idehara *et al.*, "High-Speed Frequency Modulation of a 460-GHz Gyrotron for Enhancement of 700-MHz DNP-NMR Spectroscopy," *J. Infrared Millim. Terahertz Waves*, vol. 36, no. 9, pp. 819–829, Sep. 2015, doi: 10.1007/s10762-015-0176-2.

[85] E.M. Khutoryan *et al.*, "Simultaneous Stabilization of Gyrotron Frequency and Power by PID Double Feedback Control on the Acceleration and Anode Voltages," *J. Infrared Millim. Terahertz Waves*, vol. 38, no. 7, pp. 813–823, Jul. 2017, doi: 10.1007/s10762-017-0374-1.

[86] S. Pan, C.-H. Du, Z.-C. Gao, H.-Q. Bian, and P.-K. Liu, "Electronic-Tuning Frequency Stabilization of a Terahertz Gyrotron Oscillator," *IEEE Trans. Electron Devices*, vol. 65, no. 8, pp. 3466–3473, Aug. 2018, doi: 10.1109/TED.2018.2839907.

[87] N. Kumar, U. Singh, and A. Bera, "Triode Type Coaxial Inverse Magnetron Injection Gun for 2-MW, 240-GHz Gyrotron," *IEEE Trans. Electron. Dev.*, vol. 66, no. 7, p. 6, 2019.

[88] A. Mishra, A. Bera, and M.V. Kartyikeyan, "Design of Magnetron Injection Gun for 140 GHz, 1MW Gyrotron," in *2020 IEEE International Conference on Electronics, Computing and Communication Technologies (CONECCT)*, 2020, p. 2, doi: 10.1109/CONECCT50063.2020.9198459.

[89] I.G. Pagonakis *et al.*, "Triode magnetron injection gun for the KIT 2 MW 170 GHz coaxial cavity gyrotron," *Phys. Plasma*, vol. 27, p. 9, 2020.

[90] F.J. Scott, "Frequency-agile gyrotron for electron decoupling and pulsed dynamic nuclear polarization," *J. Magn. Reson.*, vol. 289, p. 45–54, 2018, doi: 10.1016/j.jmr.2018.02.010.

[91] A.P. Fokin *et al.*, "Control of sub-terahertz gyrotron frequency by modulation-anode voltage: Comparison of theoretical and experimental results," *Rev. Sci. Instrum.*, vol. 90, no. 12, p. 124705, Dec. 2019, doi: 10.1063/1.5132831.

[92] M.Y. Glyavin *et al.*, "Frequency Stabilization in a Sub-Terahertz Gyrotron With Delayed Reflections of Output Radiation," *IEEE Trans. Plasma Sci.*, vol. 46, no. 7, pp. 2465–2469, Jul. 2018, doi: 10.1109/TPS.2018.2797480.

[93] M.Y. Glyavin, G.G. Denisov, M.L. Kulygin, and Y.V. Novozhilova, "Stabilization of gyrotron frequency by reflection from nonresonant and resonant loads," *Tech. Phys. Lett.*, vol. 41, no. 7, pp. 628–631, Jul. 2015, doi: 10.1134/S106378501507007X.

[94] A.A. Bogdashov, M.Y. Glyavin, R.M. Rozental', A.P. Fokin, and V.P. Tarakanov, "Narrowing of the Emission Spectrum of a Gyrotron with External Reflections," *Tech. Phys. Lett.*, vol. 44, no. 3, pp. 221–224, Mar. 2018, doi: 10.1134/S1063785018030069.

[95] I.V. Zotova, G.G. Denisov, N.S. Ginzburg, A.S. Sergeev, and R.M. Rozental, "Time-domain theory of low-Q gyrotrons with frequency-dependent reflections of output radiation," *Phys. Plasma*, vol. 25, no. 1, p. 013104, Jan. 2018, doi: 10.1063/1.5008666.

[96] M.M. Melnikova, A.V. Tyshkun, A.G. Rozhnev, and N.M. Ryskin, "Theoretical Analysis of Gyrotron Self-Injection Locking by Delayed Reflection," in *2018 43rd International Conference on Infrared, Millimeter, and Terahertz Waves (IRMMW-THz)*. Nagoya: IEEE, Sep. 2018, pp. 1–2, doi: 10.1109/IRMMW-THz.2018.8510318.

[97] M.M. Melnikova, A.B. Adilova, and N.M. Ryskin, "Using Reflections for Suppressing Parasitic Oscillation in a Multimode Gyrotron," in *2019 44th International Conference on Infrared, Millimeter, and Terahertz Waves (IRMMW-THz)*. Paris, France: IEEE, Sep. 2019, pp. 1–2, doi: 10.1109/IRMMW-THz.2019.8874071.

[98] A.P. Fokin *et al.*, "High Cyclotron Harmonics Excitation in Multi-beam Terahertz Range Gyrotrons," in *2019 PhotonIcs & Electromagnetics Research Symposium - Spring (PIERS-Spring)*. Rome, Italy: IEEE, Jun. 2019, pp. 2636–2639, doi: 10.1109/PIERS-Spring46901.2019.9017415.

[99] A. Kuleshov *et al.*, "Low-Voltage Operation of the Double-Beam Gyrotron at 400 GHz," *IEEE Trans. Electron Devices*, vol. 67, no. 2, pp. 673–676, Feb. 2020, doi: 10.1109/TED.2019.2957873.

[100] T. Idehara, S. P. Sabchevski, M. Glyavin, and S. Mitsudo, "The Gyrotrons as Promising Radiation Sources for THz Sensing and Imaging," *Appl. Sci.*, vol. 10, no. 3, p. 980, Feb. 2020, doi: 10.3390/app10030980.

[101] M. Hruszowiec *et al.*, "The Microwave Sources for EPR Spectroscopy," *J. Telecomm. Inf. Technol.*, no. 2, pp. 18–25, Jul. 2017, doi: 10.26636/jtit.2017.107616.